Thermal Properties of Alkali Bis(pentafluoroethylsulfonyl)amides and Their Binary Mixtures

Keigo Kubota, Toshiyuki Nohira, and Rika Hagiwara*

Graduate School of Energy Science, Kyoto University Sakyo-ku, Kyoto 606-8501, Japan

Thermal properties of alkali bis(pentafluoroethylsulfonyl)amides, MPf_2N (M = Li, Na, K, Rb, and Cs), and their binary mixtures have been revealed. Phase diagrams have been constructed for 10 binary systems, and their eutectic compositions and temperatures have been determined. It was found that the molten salt electrolytes with melting points in the intermediate temperature range (450 to 650) K are easily formed by mixing two kinds of single MPf_2N salts.

Introduction

Molten salts have excellent characteristics as electrolytes, such as negligibly small volatility, nonflammability, high electrochemical stability, high thermal stability, and high ionic conductivity.[1,2] The authors have been exploring a new class of molten salts that possesses excellent properties as electrolytes. In our previous study, we focused on alkali metal bis(trifluoromethylsulfonyl)amides, MTf_2N (M = Li, Na, K, Rb, and Cs), and revealed the thermal and physicochemical properties of single salts as well as binary and ternary mixtures.[3−5] Although MTf_2N single salts have relatively high melting points (typically over 473 K), it was found that binary[3] and ternary[4] mixtures possess reasonably low melting points (typically (390 to 423) K).

The bis(pentafluoroethylsulfonyl)amide anion, Pf_2N^-, has been reported to possess similar properties as Tf_2N^-, such as high conformational flexibility and strong delocalization.[6] However, for alkali bis(pentafluoroethylsulfonyl)amides, MPf_2N (M = Li, Na, K, Rb, and Cs), only the melting and thermal decomposition temperatures of $LiPf_2N$ have been reported.[7,8] In relation to the study on lithium batteries, it was reported that $LiPf_2N$ dissociates in polar solvents or polymers to give lithium-conducting electrolytes.[9−11] Other properties and applications have not been reported for MPf_2N salts.

MPf_2N melts are expected to have thermal and electrochemical stabilities similar to those found for MTf_2N salts from the similarity of their anionic structures. For instance, cathode limit reactions of these melts are expected to be depositions of alkali metals because they consist entirely of alkali metal cations and electrochemically stable Pf_2N^- anions. Thus, these melts are promising electrolytes for electrochemical devices which need alkali metal deposition, such as lithium secondary batteries and sodium secondary batteries. As the first step to evaluate the feasibility of MPf_2N melts, it is important to reveal their thermal properties such as melting and decomposition temperatures for both single salts and binary mixtures. In this study, the thermal properties of single MPf_2N (M = Li, Na, K, Rb, and Cs) salts and their binary mixtures were systematically investigated to construct phase diagrams and determine eutectic compositions and temperatures.

* Corresponding author. E-mail: hagiwara@energy.kyoto-u.ac.jp.

Experimental Section

Bis(pentafluoroethylsulfonyl)imide, HPf_2N (Central Glass Co., Ltd., 70.5 % aqueous solution), Na_2CO_3 (Wako Pure Chemical Industries, mass fraction purity $w = 0.995$), K_2CO_3 (Wako Pure Chemical Industries, mass fraction purity $w = 0.999$), Rb_2CO_3 (Wako Pure Chemical Industries, mass fraction purity $w = 0.999$), and Cs_2CO_3 (Aldrich, mass fraction purity $w = 0.999$) were used for the syntheses of MPf_2N salts. $LiPf_2N$ (Central Glass Co., Ltd., mass fraction purity $w = > 0.990$) was used as received. MPf_2N (M = Na, K, Rb, and Cs) were synthesized by the following reactions.

$$2HPf_2N + M_2CO_3 \rightarrow 2MPf_2N + CO_2 + H_2O \quad (1)$$

These reactions were performed in water at room temperature.

Transition and thermal decomposition temperatures of single MPf_2N salts and their mixtures were measured by a differential scanning calorimeter DSC-60 (Shimadzu Co., Ltd.) and thermogravimeter DTG-60/60H (Shimadzu Co., Ltd.), respectively. All of the samples were packed in an aluminum cell and measured under N_2 atmosphere. For all of the samples, the scanning rate was 10 $K \cdot min^{-1}$ in the first scan, and the approximate transition temperatures were determined as the points of intersection of the baseline of the DSC curve with the tangent of the endothermic peak. The scanning rate was slowed from (10 to 2) $K \cdot min^{-1}$ when necessary. To determine the phase-transition temperatures more precisely, the second scan was performed by the stepwise heating method at intervals of 2 K. The binary phase diagrams were constructed by plotting the temperatures of endothermic peaks in the stepwise heating method against the compositions of the salts. The measurements were performed at every 0.10 mole fraction of the component salts for the entire compositional range. As for the $LiPf_2N + KPf_2N$ system, further detailed measurements were performed at every 0.05 mole fraction for the regions near the eutectic composition. In this study, inaccuracies of composition and temperature for each measurement were within ± 0.01 mole fraction and ± 2 K.

Results and Discussion

Melting and Thermal Decomposition Temperatures of Single MPf_2N Salts. Figure 1 shows the DSC curves of MPf_2N single salts. For Na, K, Rb, and Cs salts, there are endothermic

10.1021/je900902z
Published on Web 03/24/2010

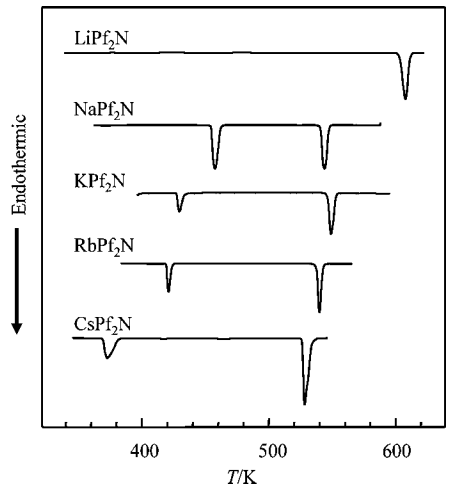

Figure 1. DSC curves of MPf_2N single salts.

Table 1. Melting Temperature, T_m, Solid−Solid Transition Temperature, T_{ss}, and Decomposition Temperature, T_d, of Single MPf_2N Salts

	T_m (this study)	T_m (previous study)	T_{ss} (this study)	T_d (this study)	T_d (previous study)
	K	K	K	K	K
$LiPf_2N$	601	605[7], 601[8]		655	< 673[8]
$NaPf_2N$	539		454	679	
KPf_2N	546		427	690	
$RbPf_2N$	539		419	681	
$CsPf_2N$	526		369	698	

peaks caused by transitions other than for melting. Thus, they have the solid−solid phase transition before melting. The melting, solid−solid transition, and thermal decomposition temperatures of MPf_2N single salts determined in the present study are summarized in Table 1 together with the reported melting temperatures for $LiPf_2N$.[7,8] The temperatures for $LiPf_2N$ determined in this study agree well with the reported values. Figure 2 shows the plots of the melting and decomposition temperatures of the single MTf_2N's[3] and MPf_2N's against the reciprocal radii of the cations. Here the coordination numbers of the cations for MPf_2N are assumed to be the same as those for MTf_2N[12] ($LiTf_2N$: 6, $NaTf_2N$: 6, KTf_2N: 8 $RbTf_2N$: 8, $CsTf_2N$: 10). For both MTf_2N and MPf_2N salts, the melting temperature of the salt containing a smaller cation is generally higher except for Na salts. The decomposition temperature

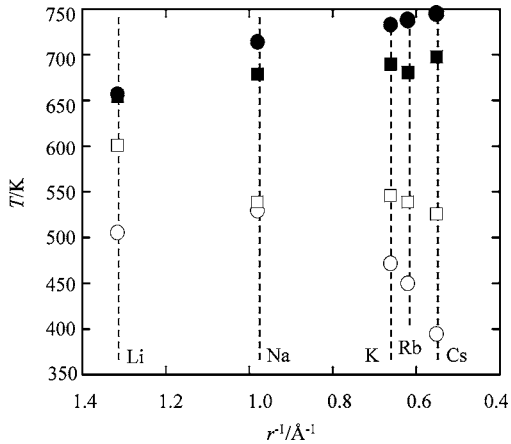

Figure 2. Plots of the decomposition temperature, T_d and melting temperature, T_m, against the reciprocal radius of the cations of the salts, r, and MPf_2N's (this study). ○, T_m of MTf_2N's (ref 3); ●, T_d of MTf_2N's (ref 3); □, T_m of MPf_2N's (this study); ■, T_d of MPf_2N's (this study).

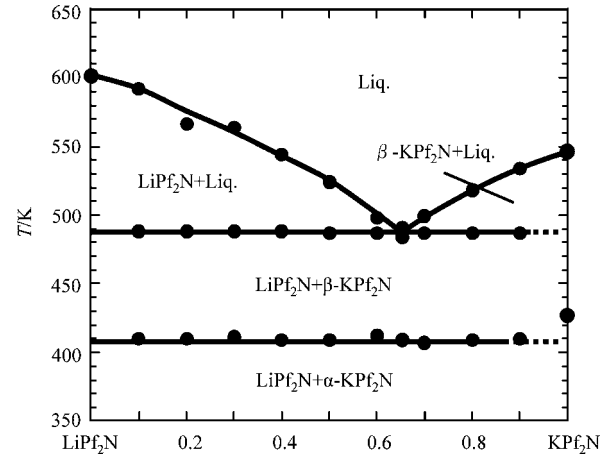

Figure 3. Phase diagram of $LiPf_2N$ + KPf_2N.

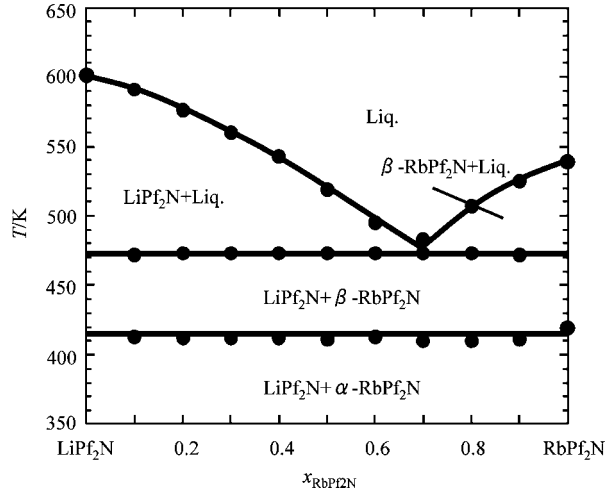

Figure 4. Phase diagram of $LiPf_2N$ + $RbPf_2N$.

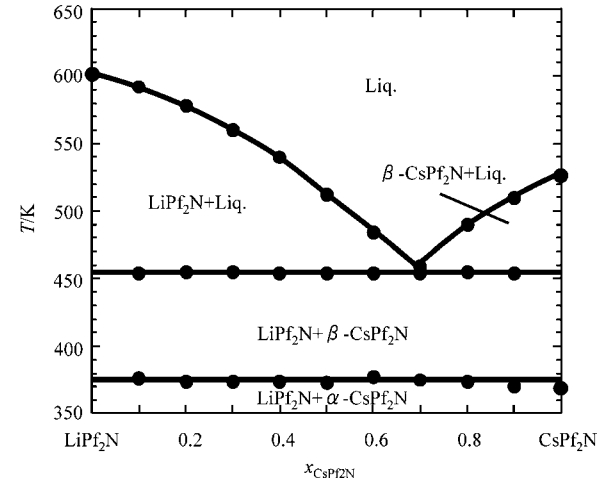

Figure 5. Phase diagram of $LiPf_2N$ + $CsPf_2N$.

becomes higher with the increase of the radius of the cation. The melting temperatures of MPf_2N salts are higher than those of MTf_2N salts of the same cation. On the other hand, the decomposition temperatures of MPf_2N and MTf_2N salts are in the same range. Thus, it is suggested that the working temperatures for MPf_2N's as molten salts are higher than those of MTf_2N's.

Phase Diagrams of the Binary MPf_2N Salt Mixtures. The binary phase diagrams were constructed for all combinations of MPf_2N salts (M = Li, Na, K, Rb, and Cs). Temperatures are

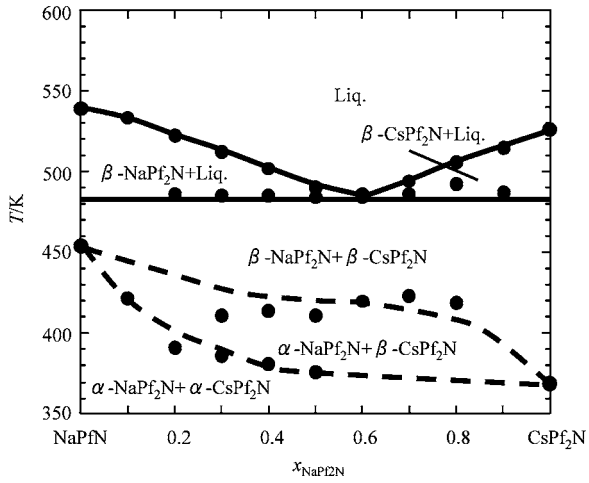

Figure 6. Phase diagram of $NaPf_2N$ + $CsPf_2N$.

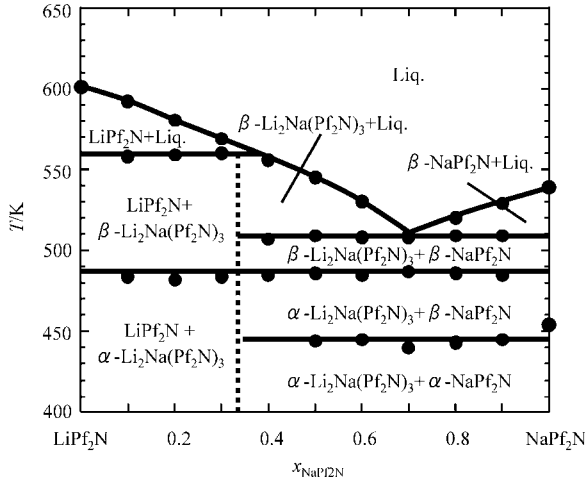

Figure 7. Phase diagram of $LiPf_2N$ + $NaPf_2N$.

Table 2. Eutectic Point, *E*, Peritectic Point, *P*, and Intermediate Compound of the Binary MPf_2N Mixtures

system	x_{MPf2N}	*T*/K	compound
$LiPf_2N$ + KPf_2N	*E*: $x_{LiPf2N} = 0.35$, $x_{KPf2N} = 0.65$	487	
$LiPf_2N$ + $RbPf_2N$	*E*: $x_{LiPf2N} = 0.35$, $x_{RbPf2N} = 0.65$	473	
$LiPf_2N$ + $CsPf_2N$	*E*: $x_{LiPf2N} = 0.30$, $x_{CsPf2N} = 0.70$	454	
$NaPf_2N$ + $CsPf_2N$	*E*: $x_{NaPf2N} = 0.40$, $x_{CsPf2N} = 0.60$	486	
$LiPf_2N$ + $NaPf_2N$	*E*: $x_{LiPf2N} = 0.30$, $x_{NaPf2N} = 0.70$	509	$Li_2Na(Pf_2N)_3$
	P: $x_{LiPf2N} = 0.60$, $x_{NaPf2N} = 0.40$	559	

given in kelvin, and the following abbreviations are used: E; eutectic point, P; peritectic point.

Figures 3, 4, and 5 show phase diagrams of the $LiPf_2N$ + KPf_2N, $LiPf_2N$ + $RbPf_2N$, and $LiPf_2N$ + $CsPf_2N$ binary systems, respectively. These phase diagrams are classified as a simple eutectic type, which has one eutectic temperature and no intermediate compound. Each binary system has a solid−solid phase transition which originates from the transition of KPf_2N, $RbPf_2N$, or $CsPf_2N$.

Figure 6 shows a phase diagram of the $NaPf_2N$ + $CsPf_2N$ binary system. This system is also a simple eutectic type. In the DSC measurements at $x_{NaPf2N} = 0.3$, 0.4, and 0.5, two endothermic peaks were observed. It is suggested that two different solid−solid phase transitions exist in this system, as shown with dashed curves in the diagram.

Figure 7 shows the phase diagram of the $LiPf_2N$ + $NaPf_2N$ binary system. The eutectic point is found at $x_{NaPf2N} = 0.70$ with the temperature of 509 K. An endothermic peak is observed at 488 K through the entire range, suggesting the existence of

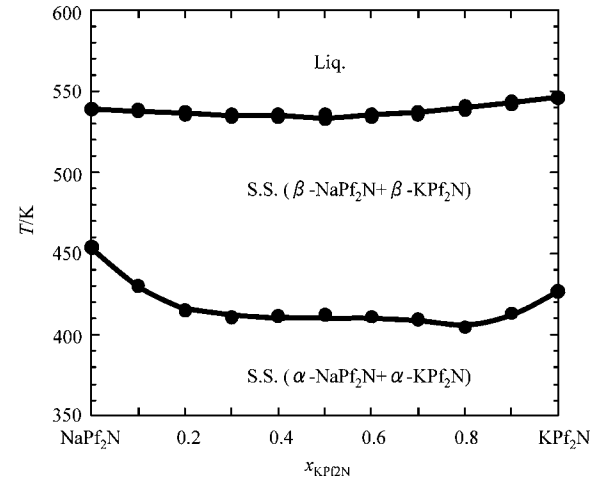

Figure 8. Phase diagram of $NaPf_2N$ + KPf_2N.

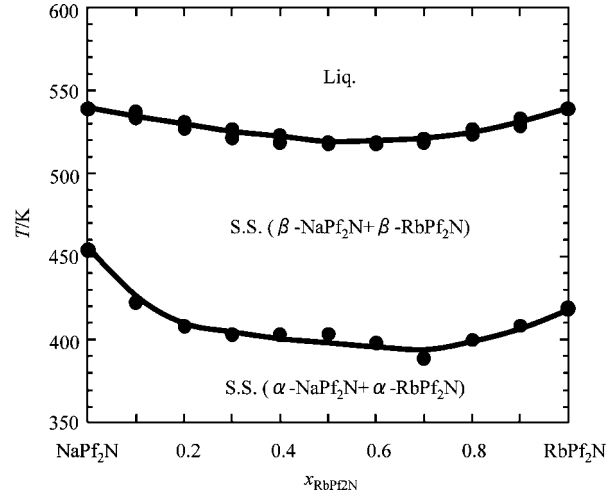

Figure 9. Phase diagram of $NaPf_2N$ + $RbPf_2N$.

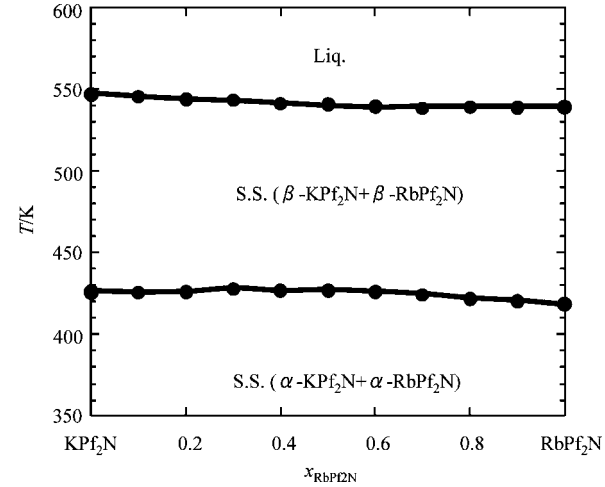

Figure 10. Phase diagram of KPf_2N + $RbPf_2N$.

the 2:1 double salt, $Li_2Na(Pf_2N)_3$, as an intermediate compound. This peak is considered to be assigned to the solid−solid phase transition of $Li_2Na(Pf_2N)_3$. There is one peritectic point at $x_{NaPf2N} = 0.40$ with the temperature of 559 K.

Table 2 summarizes the eutectic compositions and temperatures, the peritectic composition and temperature, and the intermediate compound of binary MPf_2N mixtures. In these five binary systems, eutectic temperatures ranging from (454 to 509) K are lower than those of constituent single salts. These binary

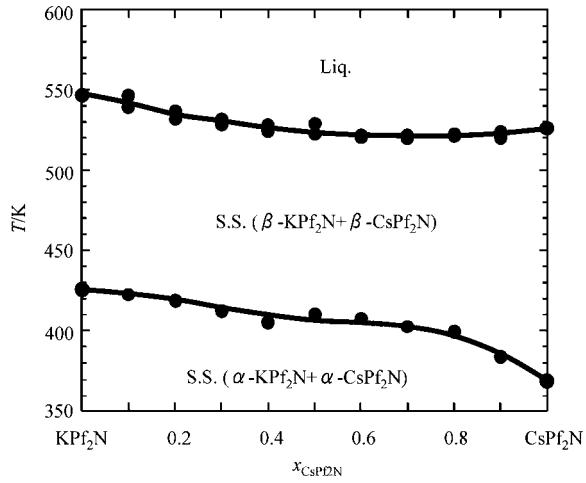

Figure 11. Phase diagram of $KPf_2N + CsPf_2N$.

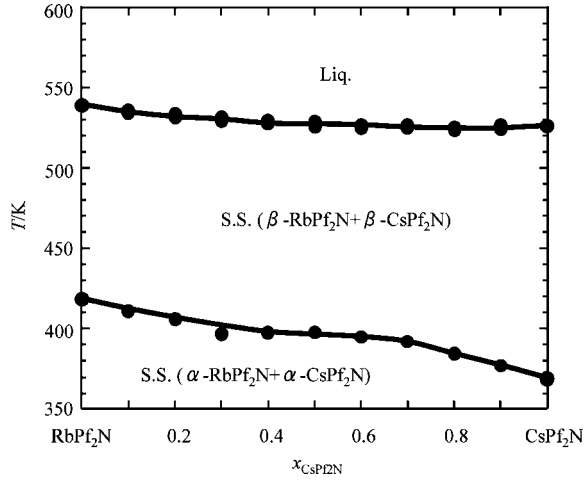

Figure 12. Phase diagram of $RbPf_2N + CsPf_2N$.

melts are expected to be useful electrolytes because of their wide liquid temperature ranges.

Figures 8, 9, 10, 11, and 12 show phase diagrams of the $NaPf_2N + KPf_2N$, $NaPf_2N + RbPf_2N$, $KPf_2N + RbPf_2N$, $KPf_2N + CsPf_2N$, and $RbPf_2N + CsPf_2N$ binary systems, respectively. Two sharp peaks are observed in the DSC curves in the entire composition range for all of these binary systems. The two peaks in each system are ascribed to solid−solid phase transition and melting, respectively. For all occasions of melting, coexistence of solid and liquid were not observed, indicating that solid solutions are formed over the entire range of composition.

According to the TG measurements, the thermal decomposition temperatures are determined by the lower decomposition temperatures of one of the constituent single salts for all of the binary mixed salts. Thus, there is no effect of mixing on the decomposition temperatures.

Conclusions

Thermal properties of single MPf_2N (M = Li, Na, K, Rb, and Cs) salts and binary mixtures were investigated. Ten binary phase diagrams have been constructed. From the viewpoint of thermal properties, some binary MPf_2N melts are expected to be more useful than single MPf_2N melts as electrolytes because of their lower melting temperatures. For MTf_2N's and MPf_2N's, the binary system possessing a large difference in the constituent cationic radii is apt to form a eutectic type.

Supporting Information Available:

Tables of data for Figures 3 to 12. This material is available free of charge via the Internet at http://pubs.acs.org.

Literature Cited

(1) Ito, Y.; Nohira, T. Non-conventional Electrolytes for Electrochemical Applications. *Electrochim. Acta* **2000**, *45*, 2611–2622.
(2) Galasiu, I.; Galasiu, R.; Thonstad, J. Electrochemistry of Molten Salts. In *Nonaqueous Electrochemistry*; Aurbach, D., Ed.; Marcel Dekker: New York, 1999; pp 461−591.
(3) Hagiwara, R.; Tamaki, K.; Kubota, K.; Goto, T.; Nohira, T. Thermal properties of mixed alkali bis(trifluoromethylsulfonyl)amides. *J. Chem. Eng. Data* **2008**, *53*, 355–358.
(4) Kubota, K.; Nohira, T.; Goto, T.; Hagiwara, R. Ternary phase diagrams of alkali bis(trifluoromethylsulfonyl) amides. *J. Chem. Eng. Data* **2008**, *53*, 2144–2147.
(5) Kubota, K.; Nohira, T.; Goto, T.; Hagiwara, R. Electrochemical properties of alkali bis(trifluoromethylsulfonyl)amides and their eutectic mixtures. *Electrochim. Acta* **2010**, *55*, 1113–1119.
(6) Grondin, J.; Talaga, D.; Lassègues, J. C.; Johansson, P.; Henderson, W. A. Spectroscopic and *ab initio* characterization of the conformational states of the bis(perfluoroethanesulfonyl)imide anion ($BETI^-$). *J. Raman Spectrosc.* **2007**, *38*, 53–60.
(7) Thokchom, J. S.; Chen, C.; Abraham, K. M.; Kumar, B. High conductivity electrolytes in the PEO_x:$LiN(SO_2CF_3)_2$-Al_2O_3 system. *Solid State Ionics* **2005**, *176*, 1887–1893.
(8) McEwen, A. B.; Ngo, H. L.; LeCompte, K.; Goldman, J. L. Electrochemical Properties of Imidazolium Salt Electrolytes for Electrochemical Capacitor Applications. *J. Electrochem. Soc.* **1999**, *145*, 1687–1695.
(9) Appetecchi, G. B.; Shin, J. H.; Alessandrini, F.; Passerini, S. 0.6 Ah Li/V_2O_5 battery prototypes based on solvent-free PEO-$LiN(SO_2CF_2CF_3)_2$ polymer electrolytes. *J. Power Sources* **2005**, *143*, 236–242.
(10) Nagasubramanian, G. Comparison of the thermal and electrochemical properties of $LiPF_6$ and $LiN(SO_2C_2F_5)_2$ salts in organic electrolytes. *J. Power Sources* **2003**, *119*−*121*, 811–814.
(11) Saito, Y.; Capiglia, C.; Kataoka, H.; Yamamoto, H.; Ishikawa, H.; Mustarelli, P. Conduction properties of PVDF-type polymer electrolytes with lithium salts, $LiN(CF_3SO_2)_2$ and $LiN(C_2F_5SO_2)_2$. *Solid State Ionics* **2000**, *136*−*137*, 1161–1166.
(12) Xue, L.; Padgett, C. W.; DesMarteau, D. D.; Pennington, W. T. Synthesis and Structures of Alkali Metal Salts of Bis[(Trifluoromethyl)sulfonyl]Imide. *Solid State Sci.* **2002**, *4*, 1535–1545.

Received for review October 28, 2009. Accepted March 8, 2010. This work was financially supported by a Grant-in-Aid for Scientific Research for Priority Area "Science of Ionic Liquids" from Japanese Ministry of Education, Culture, Sports, Science and Technology. HPf_2N and $LiPf_2N$ were provided from Central Glass Co., Ltd.

JE900902Z